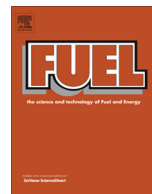




Contents lists available at SciVerse ScienceDirect

Fuel

journal homepage: [www.elsevier.com/locate/fuel](http://www.elsevier.com/locate/fuel)

## Fuel impact on the aging of TWC's under real driving conditions

Alexander Winkler<sup>a,1</sup>, Arnim Eyssler<sup>a</sup>, Alexandra Mägli<sup>b</sup>, Anthi Liati<sup>a</sup>,  
Panayotis Dimopoulos Eggenschwiler<sup>a,\*</sup>, Christian Bach<sup>a</sup>

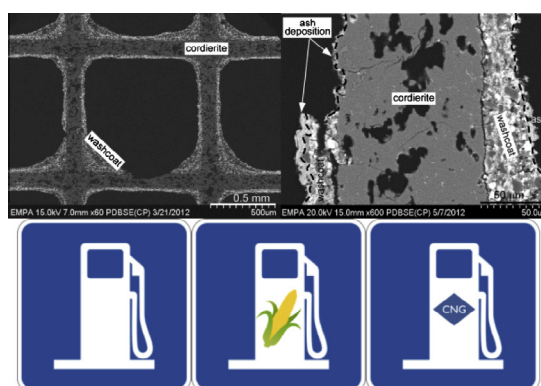
<sup>a</sup> Empa, Swiss Federal Laboratories for Materials Testing and Research, Laboratory for Internal Combustion Engines, Ueberlandstrasse 129, CH-8600 Dübendorf, Switzerland

<sup>b</sup> Empa, Swiss Federal Laboratories for Materials Testing and Research, Laboratory for Solid State Chemistry and Catalysis, Ueberlandstrasse 129, CH-8600 Dübendorf, Switzerland

### HIGHLIGHTS

- Gasoline–ethanol fuel blends result in additional mechanical and ash burden for TWCs.
- Oxidation of unburned hydrocarbons and reduction of NO<sub>x</sub> decreases.
- Catalyst ash layer of CNGs have loose 'sieve' structure.
- CNG fuel results in high HCs consisting almost entirely of CH<sub>4</sub> after catalyst.
- Ash from lube oil does not affect catalysts with CNG fuel.

### GRAPHICAL ABSTRACT



### ARTICLE INFO

#### Article history:

Received 25 February 2013  
Received in revised form 5 April 2013  
Accepted 8 April 2013  
Available online xxx

#### Keywords:

TWC  
Aging  
Gasoline  
Gasoline–ethanol blends  
Compressed natural gas (CNG)

### ABSTRACT

The impact of different fuels, gasoline, two ethanol–gasoline blends (E5, E85) and compressed natural gas (CNG), as well as lubricating oils on the aging behavior of Three-Way-Catalysts (TWCs) has been investigated with six state-of-the-art passenger cars over 40,000 km under real world driving conditions. For the study, all vehicles have been equipped with identical TWCs. During the investigation all relevant engine and vehicle operational parameters have been recorded. Exhaust gas measurements on a chassis dynamometer have been performed every 10,000 km.

After 40,000 km, the surface of the TWCs has been analyzed by means of X-ray photoelectron spectroscopy (XPS), scanning electron microscopy (SEM) and energy dispersive X-ray spectroscopy (EDX). The investigations revealed significant P, Ca, Zn and partly Mg depositions on the wash coat layer of the catalyst inlet area, rapidly decreasing along the catalyst channels towards the outlet.

The SEM images showed strongest ash depositions for the vehicles that had higher oil consumptions. Cracks and partly ablation of the wash coat at the inlet area of all TWCs have been identified strongly differing from vehicle to vehicle. Strongest damages have been encountered on the catalysts of the vehicles fuelled by the ethanol blends.

However, no emission deterioration of the vehicles could be determined over the New European Driving Cycle (NEDC) even after 40,000 km. In contrast, emission increase was ascertained over the more realistic Common Artemis Driving Cycle (CADC), which involves considerably higher space velocities of the exhaust gases through the catalysts. The vehicles using ethanol fuel blends, and having the severe damages on their wash coat layers showed the strongest emission deterioration. In contrary, vehicles with the thickest ash layer on the catalysts did not exhibit significant emission increase.

© 2013 Elsevier Ltd. All rights reserved.

\* Corresponding author. Tel.: +41 58 765 4337; fax: +41 58 765 4041.

E-mail address: [panayotis.dimopoulos@empa.ch](mailto:panayotis.dimopoulos@empa.ch) (P. Dimopoulos Eggenschwiler).

<sup>1</sup> Present address: Hug Engineering AG, Im Geren 14, 8352 Elsau, Switzerland.

## Nomenclature

### Symbols

$d$	catalyst diameter (mm)
GHSV	Gas Hourly Space Velocity ( $h - 1$ ): a measure of the average residence time of the exhaust gases in the catalyst
$g/ft^3$	gram per cubic feet: customary unit for the precious metal content of a catalyst
Hu	lower heating value of the fuel (MJ/kg)
$l$	catalyst length (mm)

### List of acronyms

BSE	back scatter electron image: modus of SEM operation
CADC	Common Artemis Driving Cycle
CLD	chemiluminescence detector: used for measuring NO <sub>x</sub> in the exhaust
CNG	compressed natural gas
cpsi	cells per square inch: customary unit for the cell density of a catalyst
E0	gasoline
E5	fuel blend (5% ethanol, 95% gasoline)

E85	fuel blend (85% ethanol, 15% gasoline)
ECE	the first part of the NEDC driving cycle, having a cold start and being similar to urban driving
EDX	energy dispersive X-ray system
EUDC	the second part of the NEDC driving cycle, being similar to rural and highway driving
FID	flame ionization detector: used for measuring unburnt hydrocarbons in the exhaust
ghg	green house gas
NDIR	non dispersive infra-red detector: used for measuring CO and CO <sub>2</sub> in the exhaust
NEDC	New European Driving Cycle
OEM	original equipment manufacturer
PGM	platinum group metals (Pt, Pd, Rh)
PM	particulate matter
SEM	Scanning electron microscopy
THC	total unburnt hydrocarbons in the exhaust
TWC	three way catalyst
XPS	X-ray photoelectron spectroscopy

## 1. Introduction

Environmental and resource depletion concerns have driven the legislation, as well as a substantial part of the research and development efforts in the automotive field in the last 20 years. Gasoline, spark-ignition engines are a relatively low-cost powertrain achieving, in combination with Three-Way-Catalysts (TWCs), very low emissions. Gasoline engines though, have rather high fuel consumption and thus high CO<sub>2</sub> emissions. Some of the latest activities in the development of gasoline powertrains occurred in the area of alternative fuels with the aim of mitigating CO<sub>2</sub> emission. Currently, the most promising alternative fuels are Ethanol and compressed natural gas (CNG).

Ethanol can be produced from biomass, resulting in reduced greenhouse gas (ghg) emissions. Additional CO<sub>2</sub> reduction and fuel efficiency gains can be obtained by targeted engine tuning for exploiting ethanol's higher octane number and flame speed. Combustion of CNG on the other hand, results in lower CO<sub>2</sub> emission per kWh energy produced, based on the advantageous C to H atoms ratio. Methane, the main constituent of CNG, has also a higher octane number compared to gasoline, thus allowing further optimization.

A series of recent studies have focused on the benefits of ethanol [1–4] with respect to engine efficiency and emissions. Ethanol has been extensively used as fuel additive, in high concentrations in some countries (Brazil, Sweden, North America) but globally in concentrations of less than 10%. Currently, some passenger cars have OEM approval for gasoline and ethanol operation. Also numerous have been the studies concerning CNG and its impact on engine performance and emissions [4–8]. In the meantime, more than 5 million CNG vehicles are in the market (figure increasing).

On the other hand, the combustion of biofuels and CNG can insert additional catalyst poisons onto the catalyst, where S and P are the elements of main concern. Especially the use of biofuels represents a potential source of additional P insertion because of the cultivation (e.g. fertilizers) and further processing route of biomass towards the fuel [9,10].

Aging phenomena and their effect on the catalytic activity have been already discussed for TWCs in combination with gasoline en-

gines [9–17] identifying thermal and chemical aging mechanisms. Thermal aging effects are caused by long term exposure of the catalysts on high temperatures and can result in sintering of the precious metal particles (PGMs) as well as of the wash coat. The former directly decreases the catalytic activity of the PGM, whereas the latter can cause collapse of the catalyst structure and encapsulation of the PGM [10,16]. Chemical aging comprises catalyst deactivation via poisoning of active centers or suppression of oxygen storage capacity [18], due to insertion of Mg, P, Ca, Zn, Si or S, which mainly originate from lubrication oil additives [19]. Similar analyses (but in lower quantity) have also been performed on Diesel Oxidation Catalysts [20,21].

Studies of TWC aging, in combination with either ethanol or CNG fuelling are, to our knowledge, scarce. In [10] the evolution of the emissions of a commercially available CNG/gasoline passenger car was tracked. The vehicle catalysts were analyzed, employing XPS, SEM and BET, and compared with new and oven aged catalysts of the same type. On the basis of the findings, an analysis of reasons for the methane-selective loss of catalytic activity was provided.

In this study, the influence of different fuels (E0, E5, E85 and gasoline) and lubricating oils on the aging of catalytic converters was investigated during 40,000 km of daily use of six passenger cars. Catalytic activity performance was assessed on a test bench every 10,000 km and X-ray photoelectron spectroscopy (XPS) analysis was used to identify and qualify the deposited elements on each catalyst surface, whilst energy-dispersive X-ray (EDX) mapping was used to depict the local distribution of these deposits. Scanning electron microscopy (SEM) images were used for further characterization of possible progress of thermal aging.

## 2. Experimental

### 2.1. Vehicles

The vehicles used were state-of-the-art passenger cars (mid-size); three identical cars of Type 1 with official OEM Euro-4 approval for the fuels E0, E5 and E85, one Type 1 car with only a local

**Table 1**  
Test matrix of vehicles, fuels, lube oils, used for field-tests of 40,000 km.

Vehicle	Engine oil	Fuel	Car type	Engine disp. (cm <sup>3</sup> )	Vehicle weight (kg)
Veh1	Oil 1	E0	Type 1	1798	1895
Veh2	Oil 1	E5	Type 1	1798	1895
Veh3	Oil 1	E85	Type 1	1798	1895
Veh4	Oil 1	CNG (+E0)	Type 1	1798	1895
Veh5	Oil 2	CNG (+E0)	Type 2	1984	2090
Veh6	Oil 3	CNG (+E0)	Type 2	1984	2090

**Table 2**  
Main characteristics of fuels and lube oils.

Vehicle car type	Veh1	Veh2	Veh3	Veh4	Veh5	Veh6
Mileage at start (km)	3208	3091	3584	2933	51,689	68,727
Fuel	E0	E5	E85	CNG	CNG	
H <sub>u</sub> (lower heating value) (MJ/kg)	43.04	42.26	28.6	45.8	45.8	
Ca (mg/kg)	<1	<1	<1	–	–	
Mg (mg/kg)	<1	<1	<1	–	–	
P (mg/kg)	<1	<1	<1	n.A.	n.A.	
Zn (mg/kg)	<1	<1	<1	–	–	
S (mg/kg)	6.7	6.8	<3	8.9	8.9	
Consumption (kg)	2309	2290	3321	2013	1715	1936
Lubricating oil		Oil1			Oil2	Oil3
SAE class		5W-30			0W40	5W-30
Ca (mg/kg)		2750			1090	1450
Mg (mg/kg)		<30			492	<30
P (mg/kg)		944			727	798
Zn (mg/kg)		1027			848	828
S (mg/kg)		3642			2230	2170
Cl (mg/kg)		180			<10	<10
Ash* (wt.%)		1.28			0.72	0.78
Consumption (kg)	1.061	0.829	1.491	1.648	3.613	4.389

(Swiss) approval for CNG operation and two Type 2 passenger cars with OEM Euro-4 approval for CNG.

Prior to the accumulation of 40,000 km, the original catalysts have been replaced by test catalysts of identical size ( $l = 120$  mm,

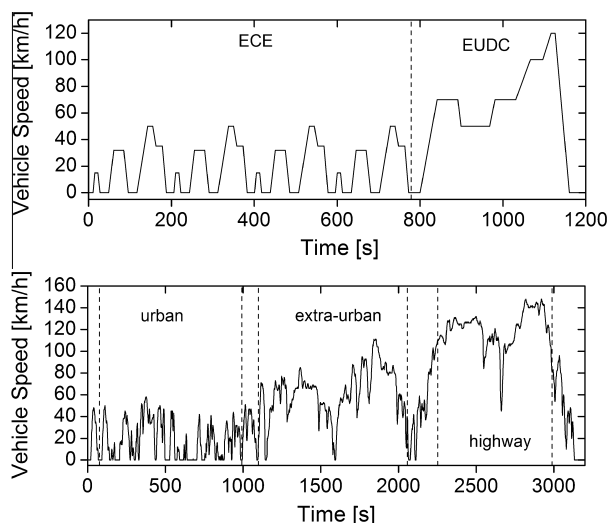


**Fig. 1.** Speed–time profiles of the New European Driving Cycle (NEDC, above) and the Common Artemis Driving Cycle (CADC below).

$d = 120$  mm, 400 cps) and composition ( $Al_2O_3$  wash coated cordierite monolith, PGM: 75 g/ft<sup>3</sup> (70 g/ft<sup>3</sup> Pd, 5 g/ft<sup>3</sup> Rh)). The new catalysts have been degreened prior to the start of the field testing.

## 2.2. Fuels and oils

The fuels used were standard-compliant gasoline (E0), 5% ethanol–gasoline (E5), 85% ethanol–gasoline (E85) blend and compressed natural gas (CNG). Three types of oil have been used: oil1: SAE 5W-40, oil2: SAE 0W-40, oil3: SAE 5W-40. In Tables 1 and 2 the combinations of engine oils, fuels and car types are shown.

## 2.3. Chassis dynamometer set-up

In order to analyze the pollutant emissions of each vehicle, two different driving cycles (NEDC and CADC) (Fig. 1) have been used on a chassis dynamometer. The NEDC is the type approval cycle specified by Council Directive 70/220–98/69/EEC (Euro-4). It consists of two parts: the cold started urban ECE (duration 780 s, maximum speed of 50 km/h) and the extra urban EUDC (duration 400 s, maximum speed of 120 km/h). The Common Artemis Driving Cycle (CADC) is the more realistic driving cycle, developed as part of an EU-funded framework five program to predict real world emissions. It consists of three parts: the hot started urban part (duration 920 s, maximum speed of 58 km/h), the rural part (duration 980 s, maximum speed of 112 km/h) and the motorway part (duration 735 s, maximum speed of 150 km/h).

The impact of the driving cycles on the catalyst operational demands is best expressed by the Gas Hourly Space Velocity (GHSV). Table 3 summarizes the mean GHSV during the NEDC and the CADC cycle. The GHSVs during the CADC are in average more than twice as high as the ones during the NEDC cycle. The larger GHSVs of vehicles 5 and 6 compared to the vehicles 1–4 can be explained by their bigger engine displacement.

## 2.4. Exhaust gas analysis

The vehicle measurements were performed on a chassis dynamometer. The exhaust gas was analyzed by NDIRs (CO and CO<sub>2</sub>), FIDs (THC, CH<sub>4</sub> and O<sub>2</sub>) and CLDs (NO/NO<sub>x</sub>), type Horriba Mexa 9400H (measurement repeatability  $\pm 1\%$ ). A CH<sub>4</sub> response factor of 1.06 was determined for the propane calibrated THC/FID-analyzer. The chassis dynamometer and its settings were applied according to the provisions of Council Directive 70/220/EEC. All measured cycles have been performed at least three times. Thus, emission results presented in the following sections are always the average of at least three consecutive measurements. Where appropriate, we have added error bars representing the standard deviation.

## 2.5. Analytical techniques

Characterization of the chemical depositions on the wash coat as well as the distribution, morphology and chemical composition of ash particulate matter (PM) in the investigated TWCs has been performed by means of X-ray photoelectron spectroscopy (XPS), optical microscopy and SEM combined with EDX for qualitative chemical analysis.

For XPS analysis, rectangular pieces of about 3 mm  $\times$  5 mm  $\times$  12 mm in size have been extracted. To ensure representative sampling over the whole catalyst, three pieces have been taken from the inlet, two from the middle, and two from the outlet. XPS spectra were acquired on a Physical Electronics (PHI) Quantum 2000 photoelectron spectrometer. Curve fitting and quantification of the detail spectra were performed with the CasaXPS software

**Table 3**  
Mean gas hourly space velocities (GHSV) of the exhaust gases in the catalysts during the NEDC and CADC driving cycles.

	Veh1	Veh2	Veh3	Veh4	Veh5	Veh6
Mean GHSV <sub>NEDC</sub> (h <sup>-1</sup> )	43,000	43,000	44,000	48,000	59,000	60,000
Mean GHSV <sub>CADC</sub> (h <sup>-1</sup> )	107,000	109,000	106,000	109,000	138,000	138,000

using the relative sensitivity factors given by the PHI MultiPak library. The spectra were referenced to the surface carbon C 1s peak at 284.8 eV as an internal standard to compensate for any charging effects.

For SEM imaging, samples were taken at the central and lateral parts of the inlet surface area of the TWCs, perpendicular to the exhaust gas flow. The samples were embedded into epoxy, to guarantee intactness of the original structure of the brittle wash coat and ash deposits and polished.

### 3. Results and discussion

#### 3.1. XPS analysis

Qualitative XPS analysis revealed that the aged catalysts were covered with depositions of P, Ca, Zn and Mg on the wash coat surface.

An overall intensity decrease of P, Ca, Zn and Mg with highest concentrations found at the monolith inlet and lowest concentrations at the exit (Fig. 2) has been detected. Among all elements, P had highest concentrations at the catalyst inlet between 6.9 and 13 at.% and was still detectable at the exit. Ca (3.1–5.8 at.%) and Zn (0.7–3.2 at.%) and Mg (0.1–6.3 at.%) were found at the inlet and almost no or very low detectable concentrations at the exit.

The overall fuel and lube oil consumptions of the vehicles have been measured throughout the reported period (Table 2) and are presented in Figs. 3 and 4. The consumed fuels (Fig. 3) are shown as split of their components (E5 = 5% E100 + 95% E0, E85 = 85% E100 + 15% E0) or as a combination of the used fuel mixes (CNG-vehicles used gasoline during cold start or as range-extender). The corresponding lower heating values are also displayed.

The oil consumption (Fig. 4) is associated with the mileage of the vehicles at the start of the investigation (before the

40,000 km test). This is clearly discernible in Fig. 4: the vehicles of Type 1 with an initial mileage of 2,933–3,584 km had an overall oil consumption of 0.829–1.648 kg, whereas the vehicles of Type 2 with higher initial mileage of 51,689 and 68,727 km had an overall oil consumption of 3.613 and 4.389 kg, respectively.

Based on the measured consumption of lube oil during 40,000 km and the analyzed oil components at the test start (Table 2) the possible total insertion of P, Mg, Ca and Zn via the lube oil was computed and related with the concentrations found by XPS analysis (Fig. 5). The dashed lines are representing the possible element insertions due to the oil consumption – neglecting possible adhesions at any inner engine parts – and the solid lines representing the comparative XPS surface concentrations. The latter are the averaged values from the analysis of the catalyst inlet, middle and exit (Fig. 2).

The overlay for the P signal shows good matching (Fig. 5) for Veh1, Veh4, Veh5 and Veh6, those vehicles powered by gasoline or compressed natural gas. The higher P-concentrations found on the catalyst surface of Veh2 and Veh3 can be explained by traces of P in biofuels (E5, E85). The measured P-concentration of E5 and E85 was below the detection limit of 1 mg/kg (Table 2). Assuming a concentration of only 0.2 mg/kg and considering the overall fuel consumption, addition P-insertions of 0.46 g and 0.66 g can be considered for Veh2 and Veh3 respectively. Unlike P and Mg, the XPS graph of Zn and Ca exhibit significantly less similarity to the theoretical possible element concentrations. When considering the Zn curve it is striking that Veh4 and 6 have significantly lower Zn-loadings on the washcoat surface, as compared to the Veh1–3 and 5.

Besides the discussed possibilities of (i) extra element insertion via the fuel, (ii) element removal due to thermal effects and (iii) different deposition mechanisms (for Ca and Zn), one has to consider the possibility of (iv) enhanced element insertion because

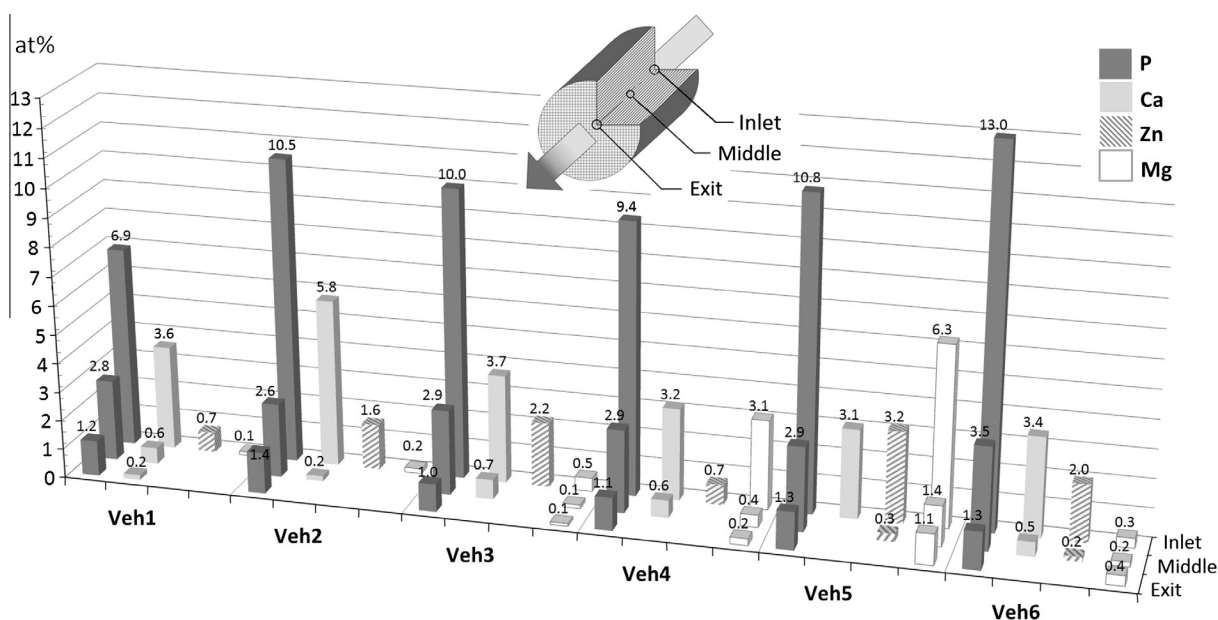
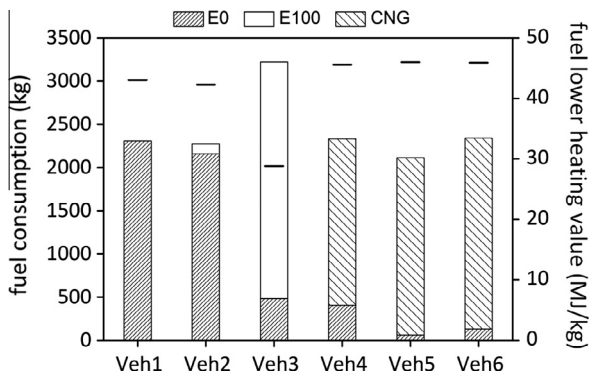
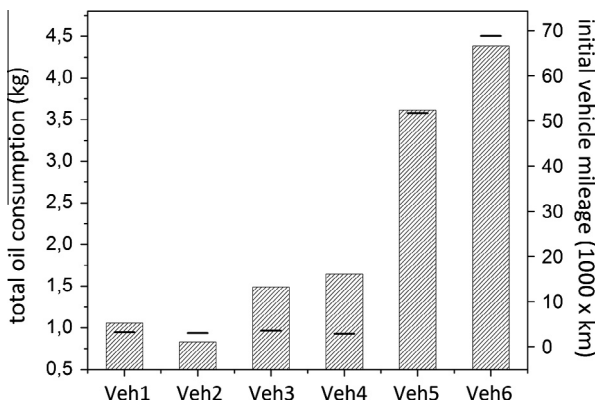


Fig. 2. XPS-analyses of P, Ca, Zn and Mg measured at the front, middle and exit of the TWC surface of each vehicle.



**Fig. 3.** Overall fuel consumption (bars) of the test vehicles split into their components in comparison with their resulting fuel heating value (black lines). Veh4 used gasoline always during cold starts and Veh5 and 6 only when ambient temperature was below 15 °C.



**Fig. 4.** Overall consumption of lubricating oil during 40,000 km (grey bars) depending on the individual vehicle mileage at the start of the test (black lines).

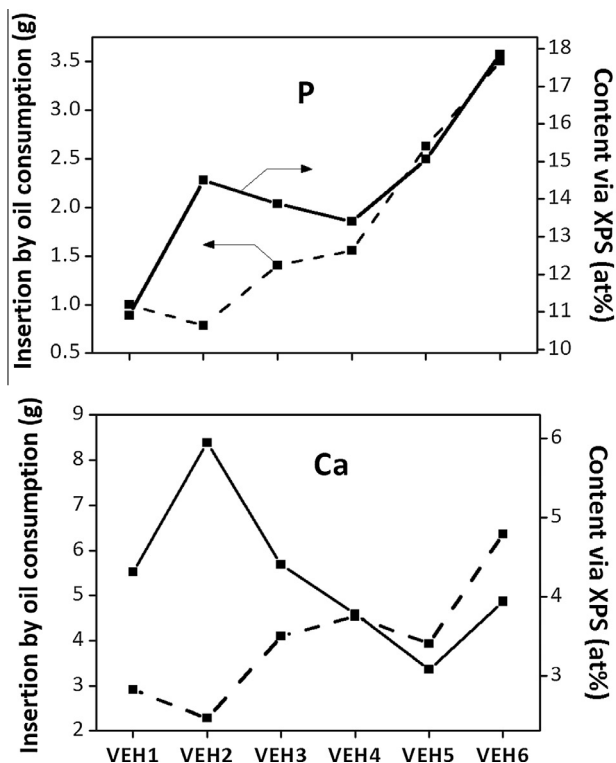


**Fig. 5.** Comparison of the absolute possible insertion of P, Mg, Ca and Zn by oil consumption (dashed line) and their aggregated surface concentrations measured by XPS (solid line).

of selective element extraction from the lube oil. Liquid injected fuels (E0, E5 and E85) mix with the lube oil and alter its consistency during operation.

### 3.2. Optical microscopy

Under the optical microscope, ash is distinguished by its brownish-beige color (Fig. 6A). In all six TWCs, the highest ash depositions occur within the first ca. 1.5 cm from inlet. Further downstream, the ash amount diminishes rapidly and becomes negligible already at the middle part of the 12 cm long TWCs. These results are in line with the decrease in ash elements found via XPS analysis.

Interestingly, the TWC of the E0-vehicle exhibits, besides ash, significant soot deposition on the inlet surface (Fig. 6B and C), most probably due to uncertainties of the  $\lambda$ -sensor. Soot deposits, intermingled with ash, are observed within the TWC channels for a few millimeters from inlet. Note that in Fig. 6B, a small part of the TWC inlet surface area was scratched off (lower left side) to reveal the soot-free surface and thus allow optical comparison with the black, soot-bearing part.

### 3.3. SEM imaging

SEM imaging was applied in order to: (i) trace in detail to what extent the wash coat of the different TWCs remained intact during operation, (ii) examine the amount and morphology of deposited ash particulate matter (PM), which may correlate with the catalytic activity of the TWC and to (iii) determine the chemical composition of the ash by use of EDX analysis. It is recalled that, in contrast to the XPS method described above, which gives information on the chemical composition of the uppermost ca. 10 nm of the ash layer, EDX data are more representative of the bulk ash chemistry, as the area analyzed is much larger in surfacial extent and depth of electron penetration. As ash depositions are largely restricted to

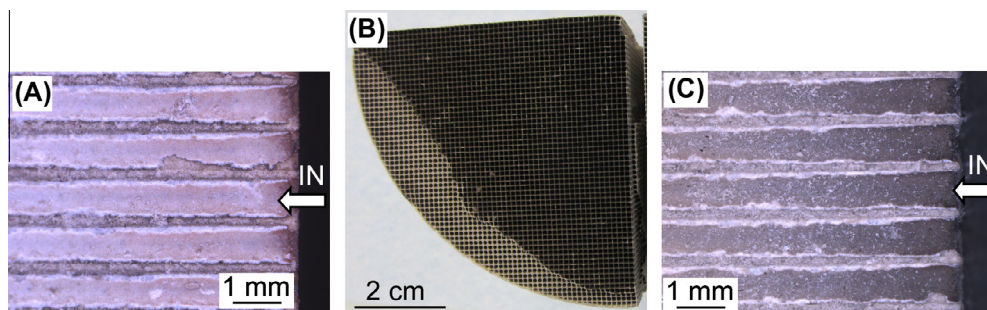


**Fig. 6.** Representative microphotographs (A and C) and photograph (B) of the inlet side of selected TWCs: (A) depicts part of the ash-rich inlet area (brownish-beige color); (B) represents a section of the soot-bearing TWC perpendicular to the flow and shows the soot-bearing inlet surface (black) and the soot-free area where soot was scratched off (lower left part). (C) Shows the soot-bearing inlet channels of the TWC operating with Vehicle 1 (E0). (A and C) represents sections parallel to the flow. (For interpretation of the references to colour in this figure legend, the reader is referred to the web version of this article.)

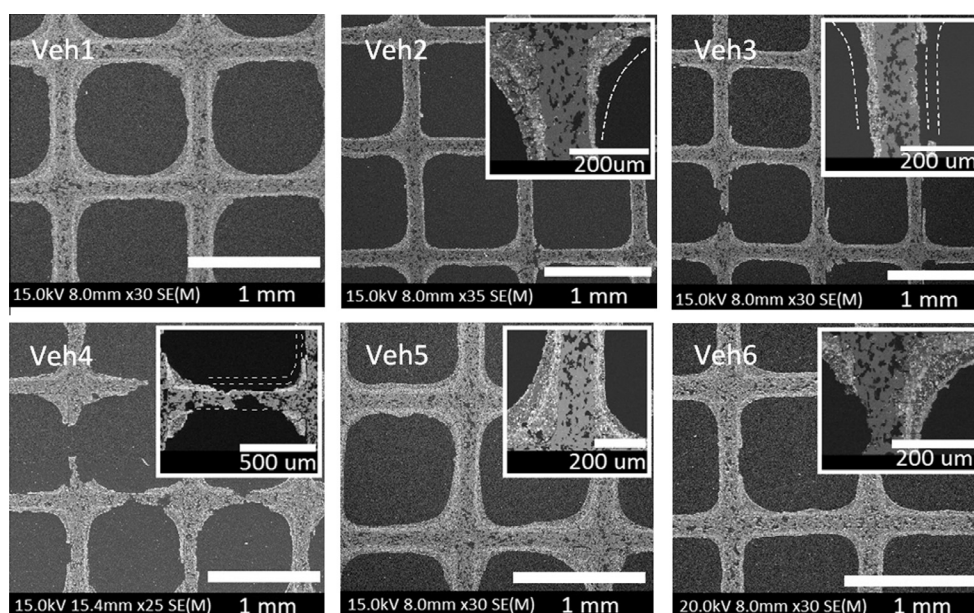


**Fig. 7.** SEM secondary electron images of representative cross sections of the aged TWCs of each vehicle (1–6). The enlarged insets emphasize the damages observed. The dashed lines outline the original extent of the upper and lower wash coat layer, as well as that of the cordierite support.

the first ca. 1.5 cm from the TWC inlet, samples for SEM studies were taken from the inlet surface, perpendicular to the exhaust gas flow, at the central and lateral parts of the TWC.

The TWC of Veh1 (E0) exhibits the most intact wash coat among all test-vehicles, however with frequent fissures, holes, and local detachment of minor parts of the outer layer. The TWCs of Veh2 and Veh3 (E5, E85) show more or less pronounced damages of their wash coat. In TWC-2, local removal of the upper wash coat layer is observed, whereas in TWC-3 both layers are missing in numerous places. TWC-3 displays even local destruction of the cordierite support in a small scale (indicated by the white arrow in Fig. 7-3). The strongest catalyst wear was found for vehicle 4. The TWC of vehicle 4 was highly damaged, not only with respect to the wash coat material, which is completely missing in large areas but also regarding the cordierite support. The strong damage of this TWC could be explained by the prevalence of unusually high temperatures due to misfiring. Finally, the TWCs of Veh5 and Veh6 demonstrate moderate damages of their wash coat, whereby the upper layer, and in rare cases also whole wash coat is partly or totally detached (inset of Fig. 7-6).

The TWCs of the vehicles 1–3 (identical lube oil-type), exhibit a relatively thin (usually 1–3  $\mu\text{m}$ , in places 3–7  $\mu\text{m}$  and in TWC-3 up to ca. 10  $\mu\text{m}$ ), compact ash layer deposited either on the wash coat

or, where the wash coat is missing, directly on the cordierite support (Fig. 7-1–3). The latter mode of occurrence of ash deposition confirms that wash coat detachment took place during engine operation and is not due to mechanical damage during, for instance, TWC sectioning and/or sample preparation. The somewhat thicker ash layer of TWC-3 is ascribed to the higher oil consumption of the vehicle (Table 2). TWC-1 and -2 show very similar ash layer thickness implying that the difference in ash production is negligible at this level of oil consumption discrepancies (Table 2).

TWC-5 and -6 are differentiated from TWC-1 to -3 in that they (a) operated with different fuel- (CNG) and lubricating oil-types and (b) showed a 3–4 times higher oil consumption (Table 2). The above distinctive features had a clear effect on the amount and chemical composition of the deposited ash and possibly also on its morphology: the ash layer in TWC-5 and -6 ranges in thickness between ca. 2 and 15  $\mu\text{m}$ , in TWC-6 reaching locally 35  $\mu\text{m}$  (in one case even ca. 50  $\mu\text{m}$ ), thus being significantly thicker than in the above described TWC-1 to -3. An interesting observation in TWC-5 and -6 is the 'sieve texture' of the ash layer (Fig. 7-5 and 6), which is different to the compact nature of the ash layer in TWC-1 to -3 (Fig. 7-2 and 3). Whether this is a primary depositional or a secondary, post-depositional feature is not clear but a detailed investigation on this issue is beyond the purpose of the

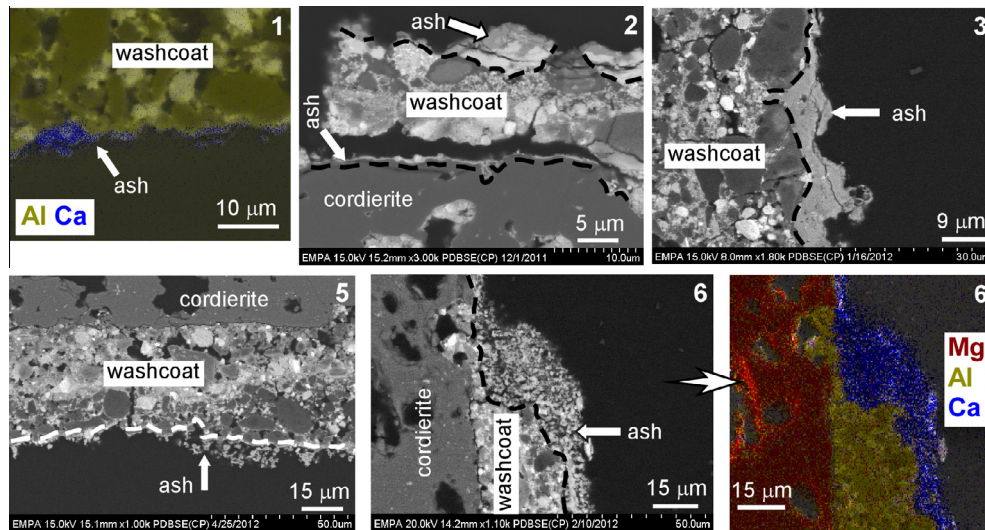


**Fig. 8.** SEM BSE images of representative parts of the TWCs studied. Numbers at the upper right corner of the images correspond to the number of the test vehicles and TWCs, as listed in Table 1. Images 1 and 6 display element mapping results, whereby Mg, Al and Ca were chosen as elements representative for the cordierite support, the wash coat and the ash layer, respectively. Dashed lines mark the limit between wash coat and ash layer, for clarity.

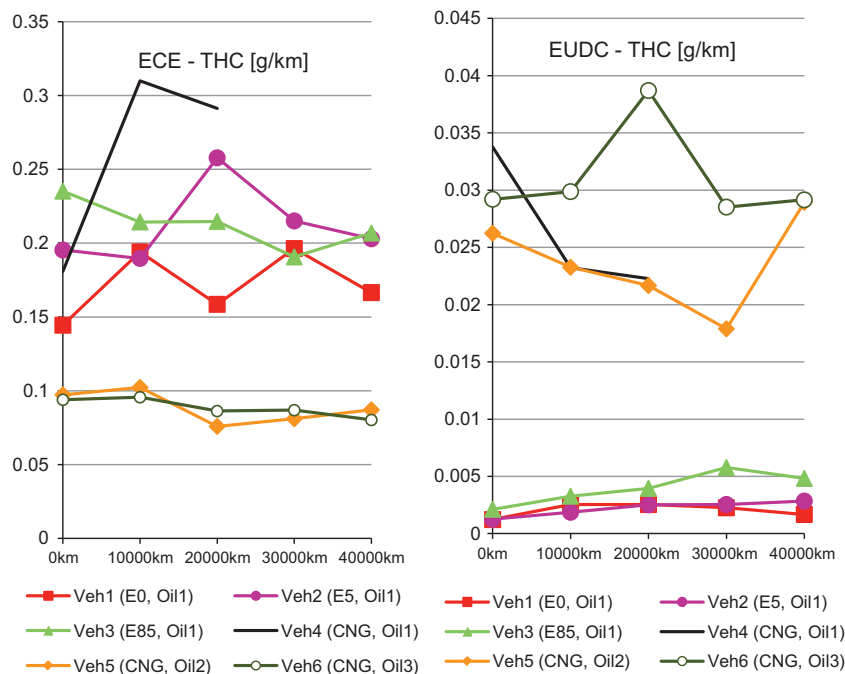


**Fig. 9.** Emission of total hydrocarbons (THC) of the vehicles over the ECE and EUDC part of the NEDC cycle during 40,000 km.

present work. Finally, no remarkable differences were found in the ash layer thickness between the central and lateral parts of the TWCs, the lateral parts showing a tendency to develop slightly thicker layers.

Qualitative EDX analysis and element mapping revealed a clear element distribution of the different TWC constituents (cordierite support, wash coat, ash; Fig. 8-1 and 6). The following composition was identified for the ash of TWC-1 to -3: Ca, P, Zn and minor amounts of Fe, Cr and Mg. Back-scattered electron (BSE) images, which have the ability to display different degrees of brightness as a function of chemical composition, reveal an inhomogeneous distribution of elements in the ash layer (Fig. 8-2). Thus, local enrichment in Zn and Fe is reflected by brighter areas of the BSE images, as these elements have a significantly higher atomic weight, compared to Ca and P, which compose mainly the grey

areas of the ash layer. These compositional differences were confirmed by EDX analysis. As a consequence of the oil-type used with TWC-5, the chemistry of the ash is significantly enriched in Mg, compared to all other TWCs but is otherwise Ca–P–Zn-bearing with lesser amounts of Fe ± Cr ± Ni ± Co, as is the case for the rest of the TWCs studied. It is noted that Fe and Cr are attributed mainly to engine wear. This inference is confirmed by element mapping, which reveals high enrichment of these elements only locally.

### 3.4. Catalysts' performances on the chassis dynamometer

#### 3.4.1. New European Driving Cycle (NEDC)

No significant changes of the emissions of the vehicles over the NEDC cycle were measured over the entire 40,000 km testing period. Veh1 (E0) exhibited some emission variations when compar-

ing the measurements at 10,000 and 20,000 km. Given though, the opposed trends among CO, THC and NO<sub>x</sub>, these variations can be attributed to uncertainties of the  $\lambda$ -sensor in the determination of the exact stoichiometric fuel-air ratio and not to catalyst aging. The emissions of Veh1, however, stabilized after 20,000 km to similar low values as in the initial tests. Veh4 (CNG), the one with the catalyst overheating between kms 20,000 and 30,000, had also similar emission instabilities. Here CO and THC emission increased over the first 20,000 km by more than a factor of two and NO<sub>x</sub> emissions decreased.

Although the NEDC results did not show any significant change over the testing period there are some interesting issues, particularly under the viewpoint that comparable vehicles have been using different fuels and identical catalysts. As expected, the emissions of Veh1 (E0) and Veh2 (E5) were very similar. Similar also have been the emissions of Veh3 (E85) apart from CO. Veh3 (E85) emitted less than half of the CO in respect to Veh1 (E0) and Veh2 (E5). Similarly low CO emission over the entire NEDC cycle had Veh5 (CNG) and Veh6 (CNG). Veh5 (CNG) and Veh6 (CNG)

had the most stable emission performance over the 40,000 km. Thus, it seems, that the significant thicker ash layer build up on the catalysts' surfaces as described in the previous section, did not deteriorate catalyst performance.

The total unburned hydrocarbon (THC) emission of the CNG vehicles during the NEDC cycle has been similar to the other vehicles. Since THC emissions of the CNG vehicles consist almost entirely of methane, methane emissions of the CNGs are roughly triple as much as of the vehicles with the other fuels. A more differentiated view is required though, with respect to the THC emissions, by observing the emissions of the vehicles during the two different NEDC parts, the ECE and EUDC part separately. The ECE initial part starts with a "cold" engine. As can be seen in Fig. 9, cold starting with CNG leads to extremely low THC emissions, while the vehicles starting with the liquid fuels emit at least double as much THCs. The situation is reversed under warm engine operating conditions. Here all the CNGs emit 6 times more unburnt hydrocarbons. As measurements confirmed, almost the entire THCs emitted by the CNG vehicles consist of methane, (harmless for city

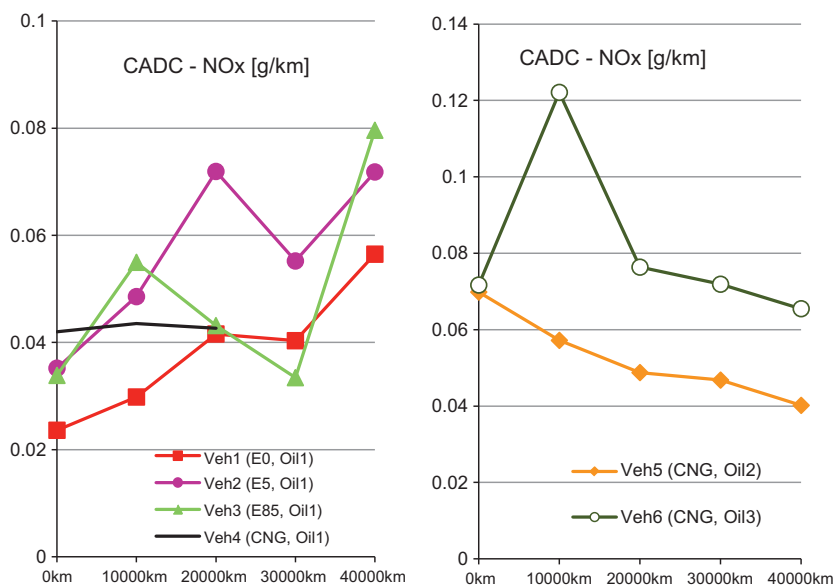


Fig. 10. NO<sub>x</sub> emissions over the CADC cycle.

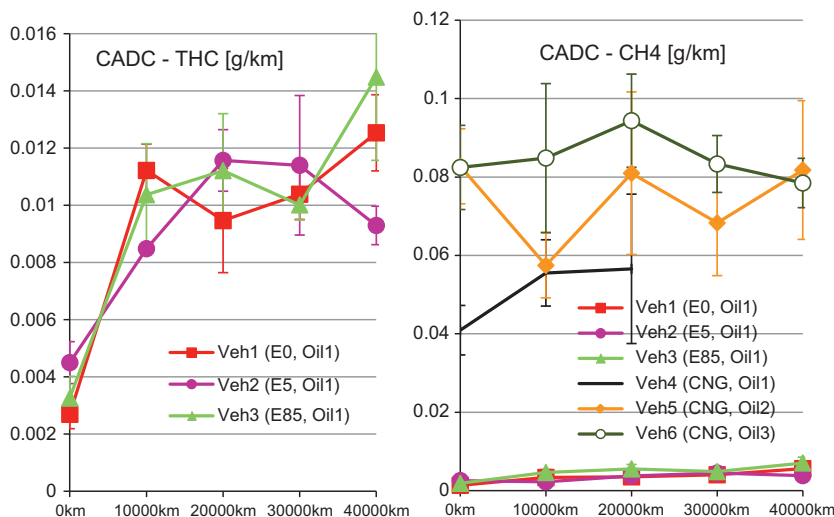


Fig. 11. THC and methane emissions over the CADC cycle (error bars represent two standard deviations).



air quality and biota, but a strong greenhouse gas). In contrast, the THCs emitted by the E0, E5 and E85 vehicles consist of max. 20% methane.

Focusing only on the EUDC part of the NEFZ cycle (Fig. 9 right diagram), incipient catalyst aging is evident for Veh2 and 3. The THC emissions of Veh1 (E0) did not change, while the emissions of Veh2 (E5) doubled and the THC emissions of Veh3 (E85) even tripled. Thus, the damages described in the previous section do affect catalyst activity, although the effect over 40,000 km is still small.

#### 3.4.2. Common artemis driving cycle (CADC)

The catalyst performance deterioration was more pronounced in the CADC cycle which is significantly more demanding (see Table 3). Regarding CO, no catalyst performance deterioration was detected. The results have been similar to those of the NEDC test, where the two CNGs and the E85 vehicle had the lowest values. Different behavior of the TWCs over time was found with regard to NO<sub>x</sub> reduction. Fig. 10 shows the NO<sub>x</sub> emissions of the vehicles in the CADC cycle. The emissions of Veh1–4 and Veh5, 6 are plotted separately. The NO<sub>x</sub> emissions of the Veh1–3 during the CADC test increased by more than a factor of two. In contrast, slight improvement of NO<sub>x</sub> emissions of the two CNG vehicles (Veh5 and 6) was found. The thick ash layer on these catalysts, as discussed in the previous section, did not affect catalyst performance not even during the CADC.

THC emissions of the Veh1–3 have more than tripled over the 40,000 km (Fig. 11, left diagram). The corresponding emissions of the CNG vehicles were rather stable over the examined period (Fig. 11 right) but at least 10 times higher in the beginning of the test. Similar trends could be observed for the methane emissions. While the methane emissions of the CNGs were almost identical to their THC emissions, the methane emissions of vehicles powered by E0, E5 and E85 were significantly lower. The methane emissions were roughly 20% of the entire THC emissions and increased similarly over the testing period.

## 4. Conclusions

XPS measurements after 40,000 km have shown high amounts of P, Ca, Zn and partly Mg on the inlet side of all catalysts. The main part of these deposits could be identified as proportional to the lube oil consumption. There have been more deposits on the catalysts of the vehicles operated with ethanol-gasoline blends than expected (based on the oil consumption). These additional deposits could be ascribed to the fuel. The deposits decreased dramatically after the first 20 mm of the catalyst inlet but were still, at least partly, detectable at the catalyst outlet. Further SEM/EDX analysis revealed:

- The E0 (gasoline) vehicle catalysts had only minor damages and only limited ash accumulation in the inlet area.
- The E5 and E85 vehicle catalysts had severely damaged wash-coat surfaces. The outer wash coat layer of the E5 catalyst was cracked and often broken with entire parts missing. The E85 vehicle catalyst had more damages. Here the outer and inner wash coat layer have been torn off the substrate at numerous locations, mainly in the inlet region.
- The catalysts of the two CNG vehicles showed the thickest ash layers on top of the wash coats, reaching at some locations 30 μm. This could be attributed to higher oil consumption. Nevertheless these ash layers appear to have a 'sieve' structure with respect to the thinner but more compact ash layers in the E0, E5 and E85 vehicles.

Concerning vehicle emission stability during the 40,000 km testing period, the following concluding remarks can be summarized:

- Despite the detected catalyst damages, no significant deterioration of vehicle emissions over the entire NEDC cycle have been measured.
- Incipient performance deterioration over the 40,000 kms can be detected with respect to the THC emissions over the "warm" EUDC part of the NEDC cycle of the E5 and E85 vehicle catalysts.
- NO<sub>x</sub> emissions during the CADC cycle increased for the E0, E5 and E85 by more than double and decreased slightly for the CNG vehicles, despite the thicker ash layer.
- THC and CH<sub>4</sub> emissions increased severely for the E0, E5 and E85 vehicles (more than tripled) during the CADC and were stable (but high) for the CNG vehicles.

Putting into focus the emission characteristics (after catalyst) of the similar vehicles operated by different fuels and equipped with identical catalysts, the following conclusions can be summarized:

- The E85 and CNG vehicles emit half, and sometimes even less, CO than the E0 and the E5.
- The CNG vehicles emit at least 5 times more THCs over the cycles examined, apart from the cold start part of the NEDC.
- Almost the entire THCs emitted by the CNG vehicles consist of methane while max. 20% of the THCs emitted by the other vehicles consists of methane.

## Acknowledgements

The authors thank Mathias Huber and Jan Stilli for their contribution on the chassis dynamometer measurements.

The authors gratefully acknowledge the Verband der Schweizerischen Schmierstoffindustrie (VSS lubes), Gasmobil AG, Schweizerischer Verein des Gas- und Wasserfaches (SVGW) Bundesamt für Umwelt (BAFU), Forschungsfonds der Erdöl-Vereinigung (FEV) and Umicore AG for their support.

SWISSGAS AG, SGS Germany, Haltermann Products and Motorex AG are also gratefully acknowledged for performing fuel and oil analysis.

## References

- [1] Park C, Choi Y, Kim C, Oh S, Lim G, Moriyoshi Y. Performance and exhaust emission characteristics of a spark ignition engine using ethanol and ethanol-reformed gas. *Fuel* 2010;89:2118–25.
- [2] Cordeiro de Melo TC, Machado GB, Belchior CRP, Colaco MJ, Barros JEM, de Oliveira EJ, et al. Hydrous ethanol-gasoline blends – combustion and emission investigations on a flex-fuel engine. *Fuel* 2012;97:796–804.
- [3] Zhuang Y, Hong G. Primary investigation to leveraging effect of using ethanol on reducing fuel consumption. *Fuel* 2013;105:425–31.
- [4] van Basshuysen R, Schäfer F. *Handbuch verbrennungsmotoren*. 2nd ed.; 2002.
- [5] Aslam MU, Masjuki HH, Kalam MA, Abdesselam H, Mahlia TM, Amalina MA. An experimental investigation of CNG as an alternative fuel for a retrofitted gasoline vehicle. *Fuel* 2006;85:717–24.
- [6] Bach C, Laemmle C, Bill R, Soltic P, Dyntar D, Janner P, et al. Clean engine vehicle: a natural gas driven euro-4/SULEV with 30% CO<sub>2</sub>-emissions. In: *SAE techn paper 2004-01-0645*.
- [7] Dimopoulos P, Rechsteiner C, Soltic P, Laemmle C, Boulouchos K. Increase of passenger car engine efficiency with low engine-out emissions using hydrogen-natural gas mixtures: a thermodynamic analysis. *Int J Hydrogen Energy* 2007;32:3073–83.
- [8] Dimopoulos P, Bach C, Soltic P, Boulouchos K. Hydrogen-natural gas blends fuelling passenger car: engines: combustion, emissions and well-to-wheels assessment. *Int J Hydrogen Energy* 2008;33:7224–36.
- [9] Franz J, Schmidt J, Schoen C, Harperscheid M, Eckhoff S, Roesch M, et al. Deactivation of TWC as a function of oil ash accumulation – a parameter study. In: *SAE technical paper 2005-01-1097*; 2005.

- [10] Winkler A, Dimopoulos P, Hauert R, Bach C, Aguirre M. Catalytic activity and aging phenomena of three-way catalysts in a compressed natural gas/gasoline powered passenger car. *Appl Catal B* 2008;84:162–9.
- [11] Zi X, Liu L, Xue B, Dai H, He H. The durability of alumina supported Pd catalysts for the combustion of methane in the presence of SO<sub>2</sub>. *Catal Today* 2011;175:223–30.
- [12] Lox ESJ, Ertl G, et al., editors. *Handbook of heterogeneous catalysis—second. Completely revised and enlarged edition.* Wiley-VCH, Verlag; 2008. p. 2274.
- [13] Twigg MV. Progress and future challenges in controlling automotive exhaust gas emissions. *Appl Catal B* 2007;70:2–15.
- [14] Twigg MV. Catalytic control on emissions from cars. *Catal Today* 2011;163:33–41.
- [15] Granados ML, Larese C, Cabello Galisteo F, Mariscal R, Fierro JLG, Fernandez-Ruiz R, et al. Effect of mileage on the deactivation of vehicle-aged three-way catalysts. *Catal Today* 2005;77(107–108):77–85.
- [16] Neyestanki AK, Klingstedt F, Salmi T, Murzin DY. Deactivation of postcombustion catalysts, a review. *Fuel* 2004;83:395.
- [17] Herbst K, Mogensen G, Huber F, Østberg M, Skjøth-Rasmussen MS. Challenges in applied oxidation catalysis. *Catal Today* 2010;157:297–302.
- [18] Christou SY, Álvarez-Galván MC, Fierro JLG, Efstathiou AM. Suppression of the oxygen storage and release kinetics in Ce<sub>0.5</sub>Zr<sub>0.5</sub>O<sub>2</sub> induced by P, Ca and Zn chemical poisoning. *Appl Catal B: Environ* 2011;106:103–13.
- [19] Armstrong DR, Ferrari ES, Roberts KJ, Adams D. An investigation into the molecular stability of zinc di-alkyl-di-thiophosphates (ZDDPs) in relation to their use as anti-wear and anti-corrosion additives in lubricating oils. *Wear* 1997;208:138–46.
- [20] Winkler A, Ferri D, Aguirre M. The influence of chemical and thermal aging on the catalytic activity of a monolithic diesel oxidation catalyst. *Appl Catal B* 2009;93:177–84.
- [21] Winkler A, Ferri D, Hauert R. Influence of aging effects on the conversion efficiency of automotive exhaust gas catalysts. *Catal Today* 2010;155:140–6.